GaN Microwave Electronics

Umesh K. Mishra, *Fellow, IEEE*, Yi-Feng Wu, Bernd P. Keller, Stacia Keller, and Steven P. Denbaars

***Abstract*—In this paper, recent progress of AlGaN/GaN-based power high-electron-mobility transistors (HEMT's) is reviewed. Remarkable improvement in performances was obtained through adoption of high Al contents in the AlGaN layer. The mobility in these modulation-doped structures is about 1200 cm$^2 \cdot$ V$^{-1} \cdot$ s^{-1} at 300 K with sheet densities of over 1 $\times$ 10^{13} cm^{-2}. The current density is over 1 A/mm with gate–drain breakdown voltages up to 280 V. F_t values up to 52 GHz have been demonstrated. Continuous wave (CW) power densities greater than 3 W/mm at 18 GHz have been achieved.**

***Index Terms*—FET, GaN, HEMT, microwave, transistor.**

I. Introduction

THE NEED for high-power solid-state amplifiers has exploded with the development of wireless communications. Requirements include attributes of ultrahigh power, high efficiency, linearity, manufacturability, and ultimately, low cost. Though the relative importance of each of these features is application specific, it is clear that current technologies fall short of satisfying a majority of the needs simultaneously. Furthermore, market needs are currently satisfied with a multitude of technologies, including silicon- and III–V-based solid-state solutions and the ever-advancing and increasingly reliable vacuum tube solution. Therefore, a new technology has to a large extent a difficult task, that of providing a better solution, not a unique one. Wide-bandgap semiconductors promise the potential of a single technology, which either aids conventional implementations or creates affordable new configurations. In particular, the GaN-based family of semiconductors is attractive, as it has technological and cost advantages over competing semiconductors (e.g., SiC). Firstly, GaN possesses attractive electronic material properties such as a large bandgap (3.4 eV), high breakdown field (3 $\times$ 10^6 V $\cdot$ cm^{-1}), the existence of modulation-doped AlGaN/GaN structures with attendant high electron mobility (1500 cm$^2 \cdot$ V$^{-1} \cdot$ s^{-1}) and extremely high peak (3 $\times$ 10^7 cm $\cdot$ s^{-1}) and saturation (3 $\times$ 10^7 cm $\cdot$ s^{-1}) [1]. Secondly, it has the technology development costs amortized over several large electronic and opto-electronic applications and, therefore, could potentially be a low-cost solution. In this paper, we will summarize the technology development and status of GaN-based microwave/millimeter-wave power devices.

Manuscript received November 11, 1997; revised March 4, 1998. This work was supported in part by Dr. K. Sleger, under ONR MURI, and Dr. G. Witt, under AFOSR.

U. K. Mishra, S. Keller, and S. P. Denbaars are with the Department of Electrical and Computer Engineering, University of California, Santa Barbara, CA 93106 USA.

Y.-F. Wu and B. P. Keller are with WideGap Technology, Goleta, CA 93117 USA.

Publisher Item Identifier S 0018-9480(98)04037-X.

II. Epitaxial-Materials Design and Properties

Microwave devices in the GaN-based system are presently based on designs developed in the conventional III–V semiconductors, namely the MESFET, heterostructure MESFET, and high-electron-mobility transistor (HEMT) or MODFET. The materials occur in either hexagonal or cubic forms, with the former being stable and the latter meta-stable. Hexagonal crystals are grown on sapphire or 6H/4H SiC, whereas the cubic forms are grown on polar cubic materials such as GaAs. The work on microwave transistors has currently been confined to hexagonal materials. The epitaxial materials are grown either by molecular-beam epitaxy (MBE) or metal–organic–chemical–vapor deposition (MOCVD). Of the possible device structures, the GaN MESFET, though simple to grow and process, does not afford the full advantage of the material, as the effective Schottky-barrier height to doped GaN is relatively low (<1 V) and, hence, is not preferred in anticipated high-voltage applications. AlGaN/GaN structures are attractive as both a high-mobility and high-carrier density, through a two-dimensional electron gas (2-DEG), are generated, and a high Schottky-barrier height to AlGaN is afforded. It is for this reason that most advances have been based on AlGaN/GaN devices. Recent intensive research on AlGaN/GaN HEMT's has resulted in a steady increase in power density from 1.1 W/mm at 2 GHz [2] to 1.5–1.57 W/mm at 4 GHz [3], [4] and 1.7 W/mm at 10 GHz [5]. These devices utilized AlGaN layers with Al mole fractions of 15%–17.5%, as the best 2-DEG mobility is generally achieved with an Al mole fraction of approximately 15%. Little had been done to investigate the impact of a higher Al mole fraction on power performance.

A higher Al mole fraction results in a higher bandgap of the AlGaN and, hence, a much higher composite breakdown field than the already wide-bandgap GaN. Also, the resultant larger conduction-band discontinuity (ΔE_c) improves carrier confinement, allowing a high mobility to coexist with a large carrier density. In addition to the conventional increase in ΔE_c in the AlGaN system with increasing Al content, an additional benefit exists in the hexagonal-based materials in that the positive piezo-electric charge induced in the AlGaN at the interface enhances the confining field, allowing increased charge confinement. The saturation velocity v_s, related to the carriers in the GaN channel, remains high, with little dependence on the AlGaN layer. Finally, as mentioned earlier, a higher Schottky gate barrier resulting from a higher Al content will more effectively suppress thermionic gate leakage current at elevated operation temperatures. These arguments predict higher equivalent figures of merit with a higher Al content. This has been experimentally demonstrated through improved dc and RF performances.

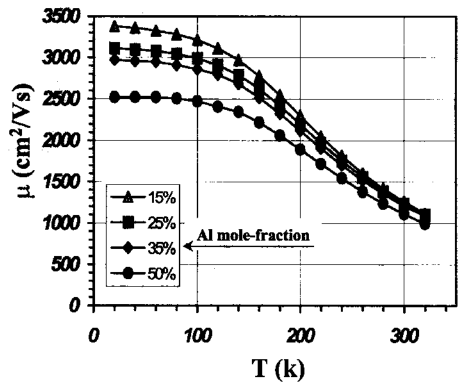

Fig. 1. 2-D gas mobility as a function temperature for various Al compositions.

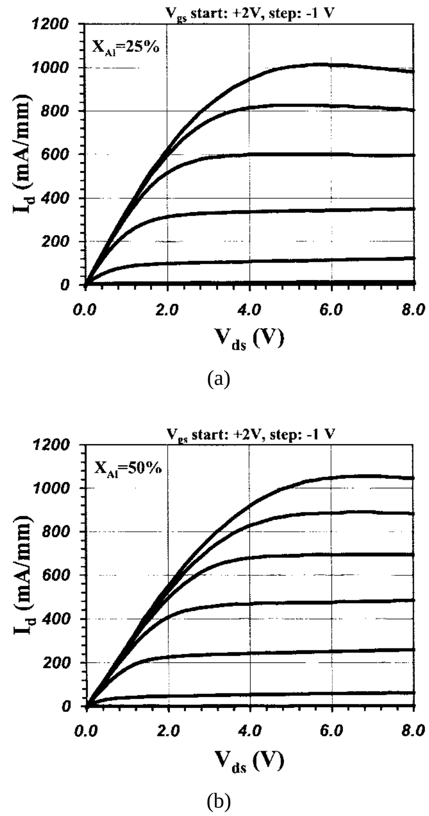

Fig. 2. DC I–V characteristics of AlGaN/GaN HEMT's with 25% and 50% Al mole fractions.

The epi-films under study were grown on C-plane sapphire substrates by MOCVD and had the same layer structure: a 200-Å GaN nucleation layer, 2-μm insulating GaN (i-GaN) and a 200-Å AlGaN donor–barrier layer. The AlGaN layer consisted of a 30-Å unintentionally doped (UID) spacer, a 150-Å Si-doped region, and a 20-Å UID cap. The Al mole fractions of the AlGaN were chosen as 15%, 25%, 35%, and 50%. Theoretically, a higher Al content leads to a larger ΔE_c and allows a higher 2-DEG density. Experimentally, the highest sheet densities achieved were 8×10^{12} cm^{-2}, 1×10^{13} cm^{-2}, 1.2×10^{13} cm^{-2}, and 1.2×10^{13} cm^{-2}, respectively. The inability to increase carrier density with X_{Al} greater than 35% is attributed to the reduced doping efficiency by Si.

Mobilities as a function of temperature are shown in Fig. 1. Each measured-sheet carrier density was essentially constant through out the temperature range of 20–320 K. The low-temperature (20 K) mobility does reduce with increasing Al content, which may be due to either the interface–roughness scattering enhanced by the higher piezo electric charge density, or the enhanced remote alloy scattering. The 300-K mobilities, however, are nearly the same, indicating that phonon scattering is dominant. For devices operating at room temperature and above, a high Al content up to 50% should introduce little increase in channel resistance.

III. Device Performance

Devices were fabricated on epi-films with Al contents of 25% and 50%. The fabrication process was a conventional mesa isolated process with chlorine reactive-ion etching (RIE) used for mesa definition. Ti/Al/Ni/Au was used for ohmic contact formation and Ni/Au for the gate metal. Transfer ohmic contact resistances were measured as 0.5 and 1 $\Omega \cdot$mm, respectively. The higher contact resistance for the latter $\mathrm{Al_{0.5}Ga_{0.5}N}$/GaN HEMT is attributed to the high Al composition of the layer. The corresponding gate lengths of the devices were 0.9 and 0.7 μm, both obtained by optical lithography. Fig. 2 shows the output I–V characteristics of both devices.

With the higher charge density of 1×10^{13} cm^{-2} compared to the $5 \sim 7 \times 10^{12}$ cm^{-2} value for the $\mathrm{Al_{0.15}Ga_{0.85}N}$/GaN devices [4], the $\mathrm{Al_{0.25}Ga_{0.75}N}$/GaN HEMT exhibited a largely increased current density of 1000 mA/mm from the previous

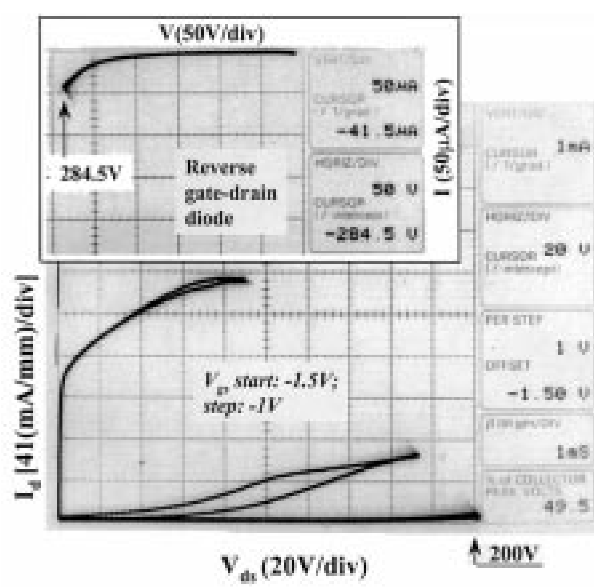

Fig. 3. High-voltage characteristics of an $\mathrm{Al_{0.5}Ga_{0.5}N}$/GaN HEMT (gate length = 0.7 μm, gate–drain spacing = 3 μm).

peak of 700 mA/mm. The on resistance was also reduced to 3 Ω·mm, resulting in a knee voltage of only 5 V for such a high current density. The much larger peak transconductance of 255 mS/mm than the previous 160 mS/mm is attributed to both the thinner AlGaN layer and the reduced access resistances. The $\mathrm{Al_{0.5}Ga_{0.5}N}$/GaN HEMT mildly suffered from the poor

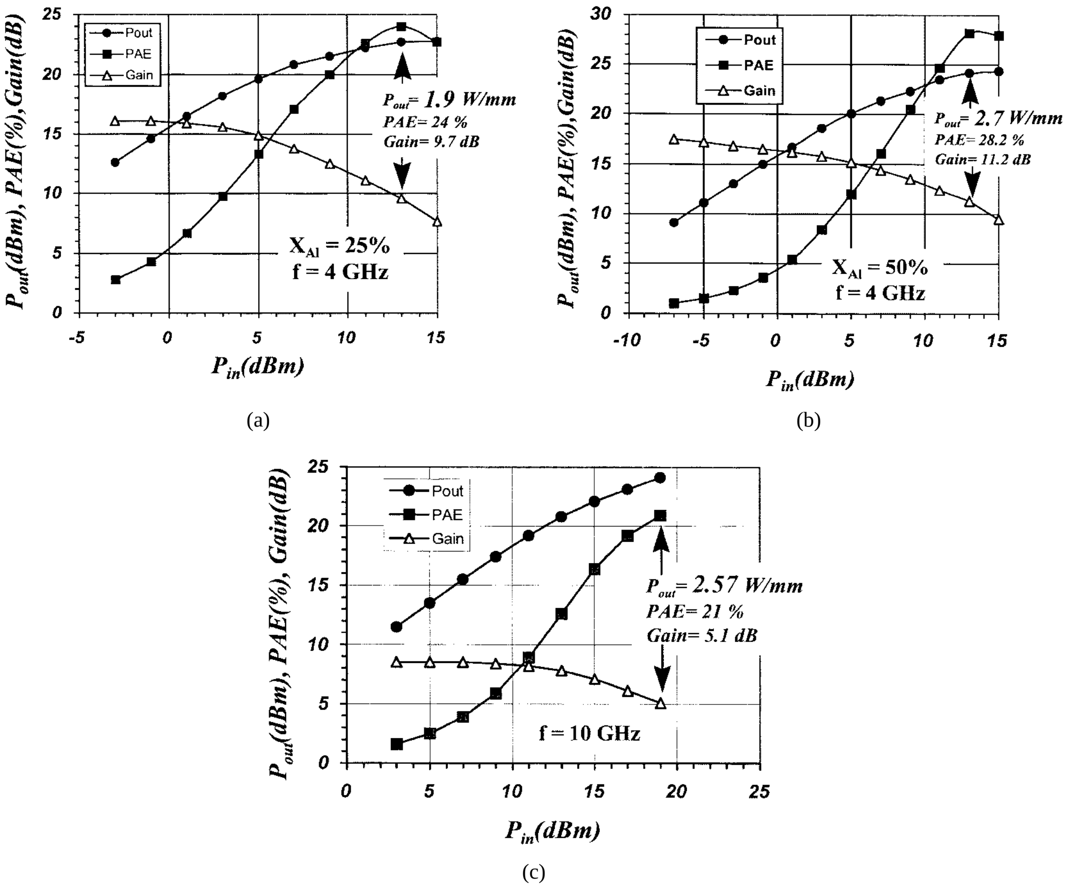

Fig. 4. Microwave power performance of the $Al_xGa_{1-x}N$/GaN HEMT's by optical lithography. (a) $X_{Al} = 25\%$, $f = 4$ GHz. (b) $X_{Al} = 50\%$, $f = 4$ GHz. (c) $X_{Al} = 50\%$, $f = 10$ GHz. Device width: 100 μm.

ohmic contact resistance. Nevertheless, with a charge density of 1.2 $\times$ 10^{13} cm^{-2}, it demonstrated a current density of 1050 mA/mm. The knee voltage is 6 V and transconductance 220 mS/mm.

Despite the much higher charge density over the previous $Al_{0.15}Ga_{0.85}N$/GaN devices [4], the $Al_{0.25}Ga_{0.75}N$/GaN HEMT's showed similar gate–drain breakdown voltages around 100, 160, and 220 V for gate–drain separations of 1, 2, and 3 μm, respectively. The corresponding values for the $Al_{0.5}Ga_{0.5}N$/GaN devices were generally 20% higher. Fig. 3 is the high-voltage I–V characteristics of an $Al_{0.5}Ga_{0.5}N$/GaN HEMT with a gate–drain spacing of 3 μm, showing a gate–drain breakdown >284 V and a three-terminal voltage >200 V before punching through. These voltages and the current density of 1 A/mm correspond to an ultrahigh I–V product per unit width of $(I_{max}V_{max}) > 200$ VA/mm. While a maximum power density of $(I_{max}V_{max})/8 = 25$ W/mm is calculated, further work needs to be done to verify this potential.

Small-signal RF measurements yielded current–gain and power–gain cutoff frequencies (f_t and f_{max}) of 15 and 35 GHz for the 0.9-μm gate-length $Al_{0.25}Ga_{0.75}N$/GaN devices, 17.5 and 44 GHz for the 0.7-μm gate-length $Al_{0.5}Ga_{0.5}N$/GaN devices, respectively. Corresponding intrinsic f_t's of 17.2 and 21.8 GHz were extracted from the S-parameters, translating to intrinsic f_t gate-length products of 15.5 and 15.3-GHz μm, considerably improved from the previous value of 11-GHz μm [4].

Continuous wave (CW) microwave power performance was characterized un-cooled on the sapphire substrate with a Maury load–pull system. As seen in Fig. 4(a), at 4 GHz, the $Al_{0.25}Ga_{0.75}N$/GaN HEMT's exhibited moderately improved output power density and power-added efficiency (PAE) of 1.9 W/mm and 24%, respectively, from the previous values of 1.57 W/mm and 20% [4]. In contrast, the $Al_{0.5}Ga_{0.5}N$/GaN devices produced a largely enhanced power density of 2.7 W/mm with a PAE of 28% and a large-signal gain of 11.2 dB [Fig. 4 (b)]. Fig. 4(c) is the measurement result of an $Al_{0.5}Ga_{0.5}N$/GaN HEMT at 10 GHz, showing a power density of 2.57 W/mm with a PAE and a large-signal gain of 21% and 5.1 dB, respectively. At 8 GHz, the corresponding values were 2.84 W/mm, 23% and 6.6 dB.

The CW power density of 2.57–2.84 W/mm up to X-band is a remarkable improvement over previous GaN-based FET's in literature. An important observation is that the current of the $Al_{0.25}Ga_{0.75}N$/GaN HEMT's degraded much more than the $Al_{0.5}Ga_{0.5}N$/GaN devices after the high-power stress up to 8.5 W/mm, which may be related to the interaction between the gate–metal and AlGaN layer. The result will be discussed in a later publication. Fig. 5 summaries the best power results measured un-cooled on sapphire substrates for various Al mole fractions. The power density monotonically increases with X_{Al}, supporting the benefit of using higher Al contents.

To take the advantage of a higher electron velocity, short gate-length $Al_{0.5}Ga_{0.5}N$/GaN devices were also fabricated.

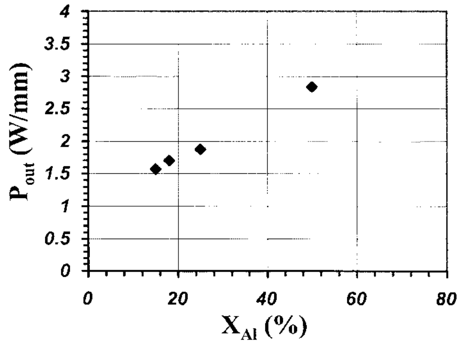

Fig. 5. Best measured output-power density versus Al mole fraction for AlGaN/GaN HEMT's by optical lithography (uncooled on sapphire substrates).

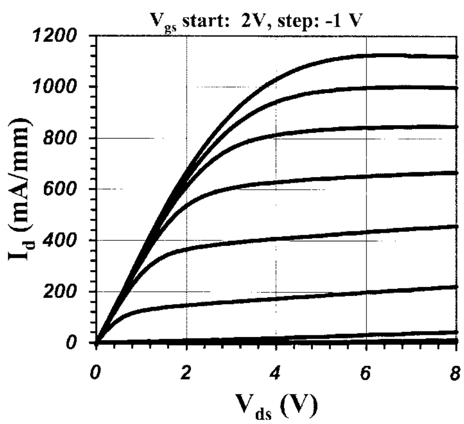

Fig. 6. I–V characteristics of a 0.25-μm gate-length $Al_{0.5}Ga_{0.5}N$/GaN HEMT.

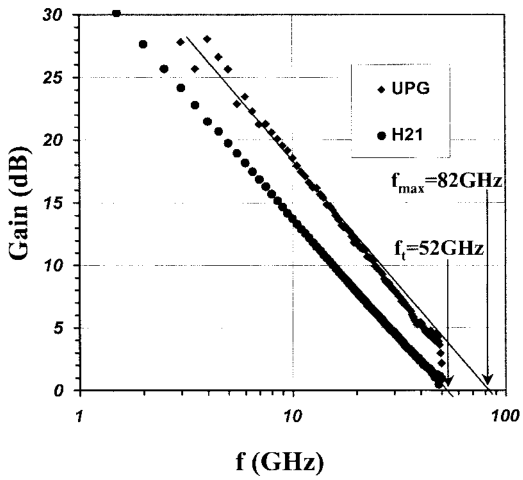

Fig. 7. Current and power gain versus frequency for a 0.25-μm gate-length $Al_{0.5}Ga_{0.5}N$/GaN HEMT (device width: 100 μm, bias: drain current = 300 mA/mm, and a source–drain voltage = 8 V).

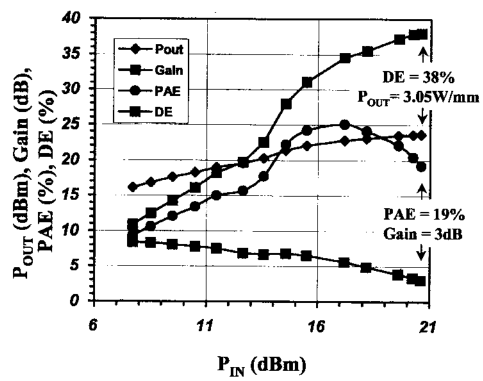

Fig. 8. Power performance of a 0.25-μm gate-length $Al_{0.5}Ga_{0.5}N$/GaN HEMT at 18 GHz (device dimension: 0.25 μm$\times$ 76 μm).

The gate definition was by electron-beam lithography with a routine T-gate technology. The gate length was 0.25–0.28 μm, while the gate–source and gate–drain separations were 0.6 and 0.75 μm, respectively. Ohmic contact resistance was measured as 0.9–1 $\Omega \cdot$mm, confirming previous result that the contact resistance of the $Al_{0.5}Ga_{0.5}N$/GaN HEMT's is higher than the 0.5 $\Omega \cdot$ mm value generally achieved with lower Al-content devices. Fig. 6 is the output I–V characteristics showing a high-saturation current density of 1130 mA/mm and a maximum extrinsic transconductance of 240 mS/mm. Both specifications are better than the 0.7-μm gate-length devices due to the shorter channel (which results in a channel velocity closer to saturation). The on-resistance is 2.85 $\Omega \cdot$ mm where the source resistance accounts for about 1.3 $\Omega \cdot$ mm. The gate–drain breakdown voltage is around 80 V. Small-signal microwave characterization performed on devices with 100-μm gatewidth yielded f_t and $f_{\max}$ of 52 and 82 GHz, respectively, as shown in Fig. 7. The f_t represents the highest reported to date for a GaN-channel FET, while the relatively low $f_{\max}/f_t$ ratio is related to the high ohmic contact resistance. An active load–pull system was used for CW power measurements. The output tuning was performed on the fundamental frequency only. The input of the device was not tuned and was connected to the microwave source with a 50-Ω line. The actual input power was calculated with the available input power and the measured input reflection coefficient (S_{11}). Fig. 8 shows the measurement result at 18 GHz for a device with a gatewidth of 76 μm, biased in class-AB mode with a drain voltage of 21 V and a quiescent drain current of 190 mA/mm (which was self-adjusted to 380 mA/mm at the maximum input drive). The small-signal linear gain is ~7.5 dB. The peak output power is 23.65 dBm, which is normalized to a power density of 3.05 W/mm. The corresponding large-signal gain, PAE, and drain efficiency (DE) are 3.1 dB, 19.2%, and 38%, respectively. Many devices with gatewidth of 76 and 100 μm showed output power densities above 3 W/mm, while the highest measured was 3.3 W/mm with a large-signal gain, PAE, and DE of 2.4 dB, 18.2%, and 42.7%, respectively. Such CW power densities are three times as high as generally achieved with GaAs MESFET's and are two times as high as those for the AlGaN/GaN devices with lower Al-contents of 15%–17% [3]–[5]. Compared with recent 4H SiC MESFET's with similar power densities at 10 GHz under pulsed condition [6], the $Al_{0.5}Ga_{0.5}N$/GaN HEMT's showed a higher operation frequency.

The effect of device width on power performance was also investigated at 8 GHz, as shown in Fig. 9. It is seen that although output power increases with increasing gatewidth,

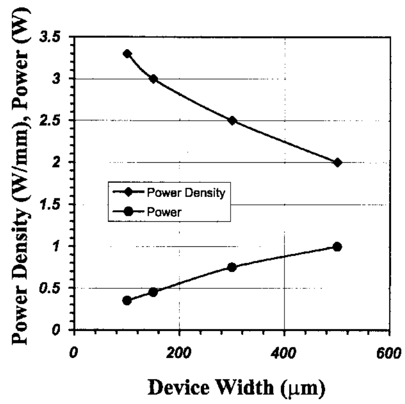

Fig. 9. Power density and total output power versus gatewidth for the 0.25-μm gate-length $Al_{0.5}Ga_{0.5}N$/GaN HEMT's at 8 GHz.

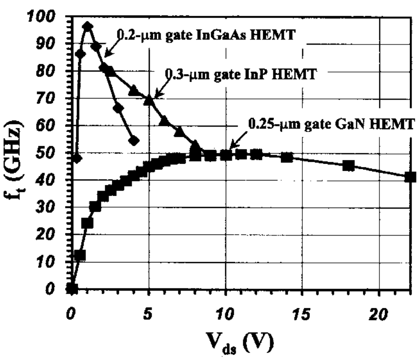

Fig. 10. Current gain cutoff frequencies versus drain bias for an $Al_{0.5}Ga_{0.5}N$/GaN HEMT (gate bias: $V_{gs} = -3$ V) as compared with GaInAs and InP channel HEMT's with similar gate lengths [7], [8].

the power density actually reduces. This is attributed to more severe self-heating for larger devices. Nevertheless, a total output power of 1 W is obtained at X-band with a 500-μm-wide device.

Finally, as a reason explaining the superior power capability at high frequencies for the GaN-channel devices, a compelling comparison, as shown in Fig. 10, is presented between the drain-bias dependence of AlGaN/GaN HEMT's versus conventional InGaAs- and InP-based HEMT's [7], [8]. As power applications require that the bias be high, it is necessary that the RF figures of merit remain high at large biases. It is clear that the f_T's of the conventional devices collapse at increased drain bias because of the drain delay in the extended depletion region, whereas f_T is maintained high in the GaN system. Though not fully understood, this suggests that the high saturation velocity of electrons in GaN may be mitigating the drain delay.

IV. Conclusions

Remarkable progress of both the AlGaN/GaN materials quality and device performance has been achieved. Within less than two years, the power density has been improved from 1.1 W/mm at 2 GHz [2] to over 3 W/mm at 18 GHz [9]. A total power of 1 W at X-band has also been demonstrated. However, several fundamental issues are unresolved. What is the nature of the GaN and AlGaN surface, why is the breakdown field strength in the highly doped two-dimensional HEMT structure approaching that predicted in undoped one-dimensional GaN, what is the electron transport physics in the HEMT and what is the best manner in which to thermally manage the device, are just a few of the questions. Nevertheless, a material system that demonstrates the high-power capability of >3 W/mm at 18 GHz in a comparatively immature stage deserves the attention to answer the questions.

Acknowledgment

The authors would like to thank C. Nguyen, N. Nguyen, M. Le, D. Grider, and P. Greiling of the Hughes Research Laboratories, Malibu, CA, and Prof. R. J. Trew, U.S. Department of Defense, Arlington, VA.

References

[1] B. Gelmont, K. Kim, and M. Shur, "Monte Carlo simulation of electron transport in gallium nitride," *J. Appl. Phys.*, vol. 74, no. 3, pp. 1818–1821, Aug. 1, 1993.

[2] Y.-F. Wu, B. P. Keller, S. Keller, D. Kapolnek, S. P. Denbaars, and U. K. Mishra, "Measured microwave power performance of AlGaN/GaN MODFET's," *IEEE Electron Device Lett.*, vol. 17, pp. 455–457, Sept. 1996.

[3] O. Akatas, Z. F. Fan, A. Botchkarev, S. N. Mohammad, M. Roth, T. Jenkins, L. Kehias, and H. Morkoc, "Microwave performance of AlGaN/GaN Inverted MODFET," *IEEE Electron Device Lett.*, vol. 18, pp. 293–295, June 1997.

[4] Y.-F. Wu, S. Keller, P. Kozodoy, B. P. Keller, P. Parikh, D. Kapolnek, S. P. Denbaars, and U. K. Mishra, "Bias dependent microwave performance of AlGaN/GaN MODFET's up to 100 V," *IEEE Electron Device Lett.*, vol. 18, pp. 290–292, June 1997.

[5] Y.-F. Wu, B. P. Keller, S. Keller, N. X. Nguyen, M. Le, C. Nguyen, T. J. Jenkins, L. T. Kehias, S. P. Denbaars, and U. K. Mishra, "Short channel AlGaN/GaN MODFET's with 50-GHz fT and 1.7-W/mm output-power at 10 GHz," *IEEE Electron Device Lett.*, vol. 18, pp. 438–440, Sept. 1997.

[6] S. Sriram, T. J. Smith, L. B. Rowland, A. A. Burk, Jr., G. Augustine, V. Balakrishna, H. M. Hobgood, and C. D. Brandt, "High power operation of 4H-SiC MESFET's at 10 GHz," in *55th Device Res. Conf.*, Boulder, CO, June 23–25, 1997.

[7] N. Moll, M. R. Heuschen, and A. Fischer-Colbrie, "Pulse-doped AlGaAs/InGaAs pseudomorphic MODFET's," *IEEE Trans. Electron Devices*, vol. 35, pp. 879–886, July 1988.

[8] O. Aina, M. Burgess, M. Mattingly, A. Meerschaert, J. M. O'Connor, M. Tong, A. Ketterson, and I. Adesida, "A 1.45-W/mm, 30-GHz InP-channel power HEMT," *IEEE Electron Device Lett.*, vol. 13, pp. 300–302, May 1992.

[9] Y.-F. Wu, B. P. Keller, P. Fini, J. Pusl, M. Le, N. X. Nguyen, C. Nguyen, D. Widman, S. Keller, S. P. Denbaars, and U. K. Mishra, "Short-channel Al0.5Ga0.5N/GaN MODFET's with power density >3 W/mm at 18 GHz," *Electron. Lett.*, vol. 33, no. 20, pp. 1742–1743, Sept. 25, 1997.

Umesh K. Mishra (S'80–M'83–SM'90–F'95) received the Ph.D. degree from Cornell University, Ithaca, NY, in 1984.

He has worked in various laboratory and academic institutions, including Hughes Research Laboratories, Malibu, CA, University of Michigan at Ann Arbor, and General Electric, Syracuse, NY, where he has made major contributions to the development of AlInAs–GaInAs HEMT's and HBT's. He is currently a Professor in the Department of Electrical and Computer Engineering, University of California at Santa Barbara. His current research interests are in oxide based III–V electronics and III–V nitride electronics and opto-electronics. He has authored or co-authored over 120 papers in technical journals and conferences and holds 5 patents.

Dr. Mishra was the recipient of the Hyland Patent Award given by Hughes Aircraft, and the Scientist of the Year Award presented at the International Symposium on GaAs and Related Compounds.

Yi-Feng Wu received the B.E. degree in engineering thermal-physics from Tsinghua University, Beijing, China, in 1985, and the M.S. degree in mechanical engineering, with emphasis in thermal science, and the Ph.D. degree, with emphasis in solid-state electronics, from the University of California at Santa Barbara, in 1994 and 1997, respectively.

From 1985 to 1993, he was with the Gaungzhou Research Institute of Nonferrous Metals, Gaungzhou, China, where he was engaged in the development of high-efficiency thermal systems. In 1995, he was began research on GaN-based microwave transistors at the University of California at Santa Barbara. He is currently a Device Researcher at WideGap Technology, Goleta, CA. He has authored or co-authored over 20 technical journal articles and conference presentations.

Bernd P. Keller received the Diploma in chemistry and the Doctoral degree from the University of Leipzig, Leipzig, Germany, in 1987 and 1992, respectively.

In 1993, he joined the Department of Electrical and Computer Engineering, University of California at Santa Barbara, as an Associate Research Engineer, where he performed research in the growth of GaN and its alloys with indium and aluminum by MOCVD. He is currently with WideGap Technology, Goleta, CA. He has authored or co-authored approximately 50 technical journal articles and conference presentations.

Stacia Keller received the Diploma and Ph.D. degree in chemistry from the University of Leipzig, Leipzig, Germany, in 1983 and 1986, respectively.

As a Scientific Assistant, she continued her experimental and theoretical work in the field of epitaxial growth of GaAs- and InP-based semiconductors at the University of Leipzig. In 1994, she joined the Electrical and Computer Engineering Department, University of California at Santa Barbara. She has published over 40 journal papers, 40 conference papers, and holds four patents. Her main research interests have been the crystal growth and characterization of group-III nitrides for electronic and opto-electronic applications.

Steven P. DenBaars received the Ph.D. degree in electrical engineering from the University of Southern California, Los Angeles, in 1988.

From 1988 to 1991, he was a Member of the technical staff in the Opoelectroncis Division, Hewlett-Packard, where he was involved in the growth and fabrication of visible LED's. He is currently an Associate Professor of materials and electrical engineering at the University of California at Santa Barbara. He has authored or co-authored over 75 technical publications, 60 conference presentation, and holds 10 patents. His current research interests are in MOCVD of III–V compound semiconductor materials and devices. Specific research interests include growth of wide-bandgap semiconductors (GaN-based), and their application to blue LED's, lasers, and high-power electronic devices.

Dr. DenBaars received the NSF Young Investigator Award in 1994.